Numerical Investigation of Transient Current Density Distributions for Multi-Ion Electrolytes at a Rotating Disk Electrode

ARTICLE *in* ANALYTICAL CHEMISTRY · OCTOBER 2004

Impact Factor: 5.64 · DOI: 10.1021/ac049804d · Source: PubMed

5 AUTHORS, INCLUDING:

Johan Deconinck
Vrije Universiteit Brussel
131 PUBLICATIONS **972** CITATIONS

Anal. Chem. **2004,** *76,* 5579−5590

Numerical Investigation of Transient Current Density Distributions for Multi-Ion Electrolytes at a Rotating Disk Electrode

Gert Floridor, Bart Van den Bossche,* Gert Nelissen, Leslie Bortels, and Johan Deconinck

Department of Electrical Engineering, Vrije Universiteit Brussel, Pleinlaan 2, 1050 Brussels, Belgium

A versatile model for the simulation of transient multiion transport and reaction processes is applied to investigate current density distributions over a rotating disk electrode for linear voltammetric sweep experiments. The model accounts for ion transport by convection, diffusion, and migration, in combination with Butler−Volmer type electrode reactions. For several process conditions (reversible and irreversible reactions, excess or lack of supporting electrolyte), the current density distribution over the disk surface is examined and the transient current response is compared to results from the more commonly used one-dimensional axial approach. The impact of migrational effects on the nonuniform local process conditions over the disk surface is illustrated, and the resulting effect on the current peak height, width, and position is investigated. A mathematical correlation for the current peak height as a function of the reacting ion transference number is established.

The rotating disk electrode (RDE) is widely used for the investigation of electrochemical reaction mechanisms in aqueous solutions. Main advantages are the small electrode surface area and the well-defined and controllable flow conditions. Even for a very small disk radius, however (1 or 2 mm), the current density distribution over the disk might become highly nonuniform, mainly depending on the applied current, electrode polarization, and electrolyte conductivity. This invokes local process conditions at the disk surface (current density, ion concentrations, electrolyte potential) that vary strongly from the disk center toward the edge. For transient processes as, for example, fast linear voltammetry and certainly pulsed current applications, this problem becomes even more critical. This explains the interest of several researchers for the rotating hemisphere electrode (RHE).[1,2] A drawback of the RHE, however, is the complex flow field, replacing the problem of a nonuniform secondary current density distribution in radial direction (as encountered for the RDE) with a nonuniform mass-transfer rate to the electrode surface.

There is a long tradition of modeling and simulating multi-ion transport and reaction (MITRe) processes at an RDE by a one-dimensional (1D) axial approach, assuming radial uniformity of process conditions in the vicinity of the electrode. Advanced MITRe models have been presented and simulated, for example, by the research groups of Feldberg,[3,4] Landolt[5,6] and Deconinck.[7,8] MITRe models in the absence of significant amounts of supporting electrolyte have been studied by Palys et al..[9,10]

Papers dealing with an axisymmetrical (AX) modeling approach for MITRe models at an RDE are more scarce, most probably due to the enhanced complexity of the numerical methods that must be applied to solve the MITRe models in two dimensions, but certainly also because of the required computer resources, often resulting in CPU times that exceed those of a one-dimensional approach by orders of magnitude. Nevertheless, Newman et al. had already presented in the 1960s a method to compute tertiary current density distributions at an RDE.[11,12] The effect of migration was treated through the concept of the concentration overpotential in the diffusion boundary layer and the Laplace equation for the electrolyte potential outside this layer (describing ohmic drop in the bulk of the solution). Electrode reaction polarization was modeled using a Butler−Volmer type expression. The theoretical problem was solved using power expansion series in the radial position for both the potential and the reacting ion concentration distribution. The results are applicable for binary electrolytes as well as for systems with an excess of supporting electrolyte. The most important simplification in this approach is the introduction of a transference number to account for the migrational influence upon the reaction ion mass

* Corresponding author. Tel.: 32-2-6293466. Fax: +32-2-6293620. E-mail: bvdbos@vub.ac.be.

(1) Matlosz, M.; Chene, O.; Landolt, D. *J. Electrochem. Soc.* **1990**, *137*, 3033.
(2) Barcia, O. E.; Lamego, L. S. R.; Mattos, O. R.; Tribollet, B. *J. Electrochem. Soc.* **2001**, *148*, C1.
(3) Stevens, N. P. C.; Rooney, M. B.; Bond, A. M.; Feldberg, S. W. *J. Physical Chem. A* **2001**, *105*, 9085
(4) Feldberg, S. W.; Goldstein, C. I.; Rudolph, M. *J. Electroanal. Chem.* **1996**, *413*, 25
(5) Zech, N.; Podlaha, E. J.; Landolt, D. *J. Electrochem. Soc.* **1999**, *146*, 2892.
(6) Bradley, P. E.; Landolt, D. *Electrochim. Acta* **1997**, *42*, 993.
(7) Dan, C.; Van den Bossche, B.; Bortels, L.; Nelissen, G.; Deconinck, J. *J. Electroanal. Chem.* **2001**, *505*, 12.
(8) Van den Bossche, B.; Floridor, G., Deconinck, J.; Van Den Winkel, P.; Hubin, A. *J. Electroanal. Chem.* **2002**, *531*, 61.
(9) Palys, M. J.; Stojek, Z.; Bos, M.; Vanderlinden, W. E. *J. Electroanal. Chem.* **1995**, *383*, 105.
(10) Palys, M. J.; Stojek, Z.; Bos, M.; Vanderlinden, W. E. *J. Anal. Chim. Acta* **1997**, *337*, 5.
(11) Hsueh, L.; Newman, J. *Electrochim. Acta* **1967**, *12*, 429.
(12) Marathe, V.; Newman, J. J. *Electrochem. Soc.* **1969**, *116*, 1704.

10.1021/ac049804d CCC: $27.50
Published on Web 08/14/2004

Table 1. Ion System Charges and Diffusion Coefficients

ion no.	name	charge	diffusion coefficient/ 10^9 m^2 s^{-1}
1	A^{2+}	+2	1
2	B^+	+1	1
3	C^+	+1	5
4	D^-	−1	1

Table 2. Ion System Bulk Concentrations c_k (mol m^{-3}) for Electrolyte Systems R and A−F

ion name	R	A	B	C	E	F	G
A^{2+}	9.95	99.5	99.5	99.5	9.95	9.95	9.95
B^+	0.1	1.0	1.0	1.0	0.1	0.1	0.1
C^+	990	9.9	99	990	0.99	9.9	99
D^-	1010	209.9	299	1190	20.99	29.9	119
σ/Ω^{-1} m^{-1}	22.6	2.48	4.49	24.6	0.248	0.449	2.46

Table 3. Values of Preexponential Rate Constants k_a and k_c for Reaction 6

reaction type	k_a/A m mol^{-1}	k_c/A m mol^{-1}
irreversible	9.95×10^{-3}	10^{-4}
reversible	9950	100

Table 4. Electrode Ion Fluxes

ion name	N_k
A^{2+}	$+j/F$
B^+	$-j/F$
C^+	0.0
D^-	0.0

transport in the diffusion boundary layer. Yen and Chapman extended this model to treat multiple electrode reactions and homogeneous reactions in the diffusion layer.[13] The ion conservation equations in the diffusion boundary layer, including the effect of migration, were solved without approximations, using an orthogonal collocation method. An important simplification in the model of Yen and Chapman is the use of one single Nernst diffusion layer thickness for distinct electroactive ions (with possibly a large variation in their diffusion coefficients). Also Baker and Verbrugge[14] used the Newman two-domain concept with a refined approach for the diffusion layer and solved migration−diffusion transport numerically after an integral transform. Durbha and Orazem extended the Newman approach by incorporating the diffuse double layer near the electrode.[15] Van den Bossche et al.[16] used a finite volume method (FVM), in combination with an upwind scheme for the convection contribution, to solve the entire system of ion conservation equations in the vicinity of an RDE. Contributions from convection, migration, diffusion, and homogeneous reactions were modeled without any reorganization or transformation of the conservation equations, in combination with Butler−Volmer type expressions for the electrode reactions. More recently, Dudek and Fedkiw[17] used the finite element method (FEM) to solve the same nonsimplified set of conservation equations, after a coordinate transformation.

Transient AX simulations for MITRe systems at an RDE—to the authors' knowledge— have only been published for a simplified set of conservation equations. Most of these papers deal with a (convective) diffusion approach, neglecting migrational effects, for example.[18,19] Part of those publications also include homogeneous chemical reactions, e.g., ref 14. Verbrugge and Baker[20] performed transient (potential step and linear sweep) numerical simulations for a three-ion system with migrational and diffusion transport near the disk electrode, but convection influences were omitted.

This paper presents simulated results for the current density distribution at an RDE for linear sweep voltammetry. The approach is based on the nonsimplified solution of the ion conservation equations, using a numerical FVM-upwind approach as presented in ref 16 and a second-order time integration scheme from ref 7. The current response from these AX simulations, in particular the peak current density, is compared to the results obtained from a one-dimensional approach,[7] for several process conditions: reversible and irreversible electrode reactions and supporting electrolyte concentrations ranging from excess to a very limited value. This allows estimation of the systematic error that is made when using the one-dimensional approach for simulating transient MITRe models.

REACTION MODEL AND MATHEMATICAL FORMULATION

Multiion Transport and Reaction Model. For all simulations performed in this paper, an exemplary four-ion system is considered (see Table 1), with A^{2+} and B^+ representing electroactive charged species and C^+ and D^- supporting electrolyte ions. A complete overview of the MITRe model as considered here can be found in ref 7. A summary is given below. Default values for the physicochemical parameters involved in this model are given in Table 1. Several sets of bulk concentrations are used, ranging from a nearly binary electrolyte to an electrolyte with an excess of supporting electrolyte (systems A−C in Table 2). System R is used for comparison with the one-dimensional simulation results from reference.[7] To investigate the influence of the ionic strength, systems D, E and F are introduced, containing the same ions as respectively systems A, B and C, but at concentrations that are 10 times lower (see Table 2.).

The total flux of each ion is formulated as

$$\bar{N}_k = -D_k \nabla \bar{c}_k + c_k \bar{v} - z_k F u_k c_k \nabla \bar{U} \qquad (1)$$

(13) Yen, S. C.; Chapman, T. J. *Electrochem. Soc.* **1987**, *134*, 1964.
(14) Baker, R. B.; Verbrugge, M. W. *J. Electrochem. Soc.* **1990**, *137*, 1832.
(15) Durbha, M.; Orazem, M. E. *J. Electrochem. Soc.* **1998**, *145*, 1940.
(16) Van den Bossche, B.; Bortels, L.; Deconinck, J.; Vandeputte, S.; Hubrin, A. *J. Electroanal. Chem.* **1996**, *411*, 129.
(17) Dudek, D. A.; Fedkiw, P. S. *J. Electroanaol. Chem.* **1999**, *474*, 31.
(18) Parikh, R. S.; Liddell, K. C. *J. Electrochem. Soc.* **1988**, *135*, 1704.
(19) Alden, J. A.; Hutchinson, F.; Compton, R. G. *J. Phys. Chem. B* **1997**, *101*, 949.
(20) Verbrugge, M. W.; Baker, R. B. *J. Phys. Chem.* **1992**, *96*, 4572.

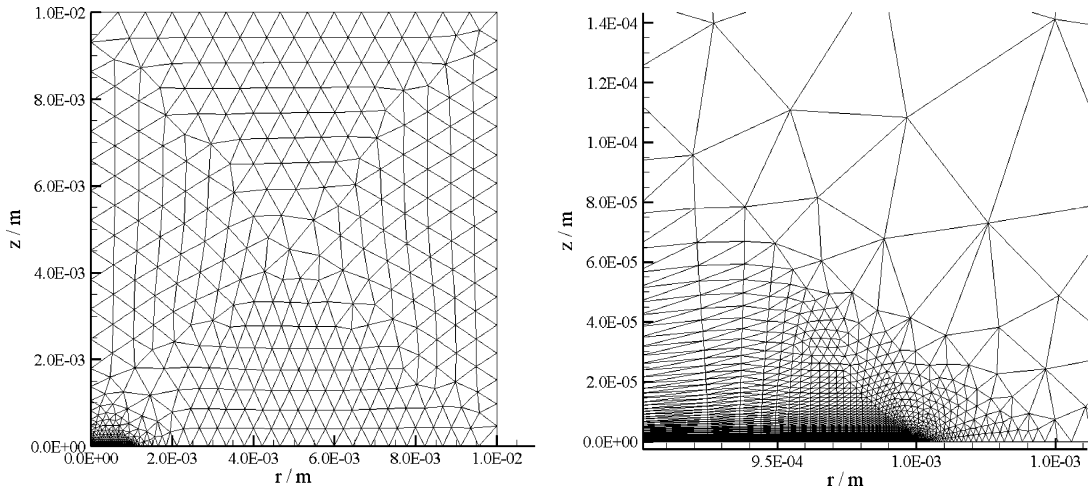

Figure 1. Hybrid triangular mesh around the RDE (axis of symmetry at $r = 0$ m, disk extending to $r = 0.01$ m). Zoom around the disk edge is plotted at the right.

Table 5. Linear Regression Coefficient *a* for Electrolyte System R

reaction type	ref	*a*	$\xi^{1/2}$
reversible	Strutwolf[28]	0.431	>5.6
	this paper 1D	0.431	>3
	this paper AX	0.425	>3
irreversible	Strutwolf[28]	0.340	>7.0
	this paper 1D	0.332	>3
	this paper AX	0.324	>3

with D_k the diffusion coefficient of ion k (m^2s^{-1}), c_k the concentration (mol m^{-3}), z_k the charge, and u_k the mechanical mobility (mol m^2 J^{-1} s^{-1}). $\bar{v}$ the vectorial fluid velocity (m s^{-1}), U the electrolyte potential (V), and F Faraday's constant (C mol^{-1}). The terms at the right describe respectively mass transport by diffusion, convection, and migration. Conservation of mass is expressed by

$$\partial c_k/\partial t = -\nabla.\bar{N}_k \tag{2}$$

where t represents time (s). The unknowns in the mass conservation equations are the ion concentrations and potential fields c_k and U. The electroneutrality condition is added to obtain a coherent set of equations:

$$\sum_{k=1}^{N} z_k c_k = 0 \tag{3}$$

When using the Nernst−Einstein relation $u_k = D_k/RT$ (with R the gas constant 8.31 J $mol^{-1}K^{-1}$) to link the ion mobility constant u_k with the ion diffusion coefficient D_k, the theoretical bulk conductivity σ (Ω^{-1} m^{-1}) of a multiion system as described by eqs 1−3 is given by[21]

$$\sigma = F^2/RT\sum_k z_k^2 D_k c_k \tag{4}$$

(21) Newman, J. *Electrochemical Systems*, 2nd ed.; Prentice Hall: Englewood Cliffs, NJ, 1991; Chapter 11.

Ions A^{2+} and B^+ are assumed to take part in a simple electrode reaction:

$$A^{2+} + e^- \leftrightarrow B^+ \tag{5}$$

This reaction is modeled by a Butler−Volmer formulation, for reversible and irreversible kinetics (see Table 3). The current density j (A m^{-2}) depends on the local reacting ion concentrations $c_{k,0}$ at the electrode surface:

$$j = k_a c_{2,0} e^{\alpha F\eta/RT} - k_c c_{1,0} e^{-\beta F\eta/RT} \tag{6}$$

where η holds for the local overpotential, expressed as the difference between electrode and adjacent electrolyte potential $V - U$. α and β are respectively the anodic and cathodic charge-transfer coefficients. and k_a and k_c are respectively the anodic and cathodic preexponential rate constants (A $mmol^{-1}$). The local ion fluxes N_k perpendicular to the electrode surface are coupled to the reaction current density j as listed in Table 4.

Since in this paper simulations are performed for electrolytes with a strongly varying amount of supporting electrolyte, the ionic strength I (mol m^{-3}) is to be defined[21]

$$I = \frac{1}{2}\sum_k z_k^2 c_k \tag{7}$$

Also, the transference number[21] τ for reacting species A^{2+} becomes an important parameter if the supporting electrolyte concentration is not present in excess compared to the bulk concentration of the A^{2+} ion:

$$\tau = z_1^2 D_1 c_1 / \sum_k z_k^2 D_k c_k \tag{8}$$

Numerical Solution Method. The numerical method that is being used in this paper to solve the system of nonlinear eqs 1−3 and 6 for the ion concentration c_k and electrolyte potential U field variables, with electrode boundary conditions as given in Table

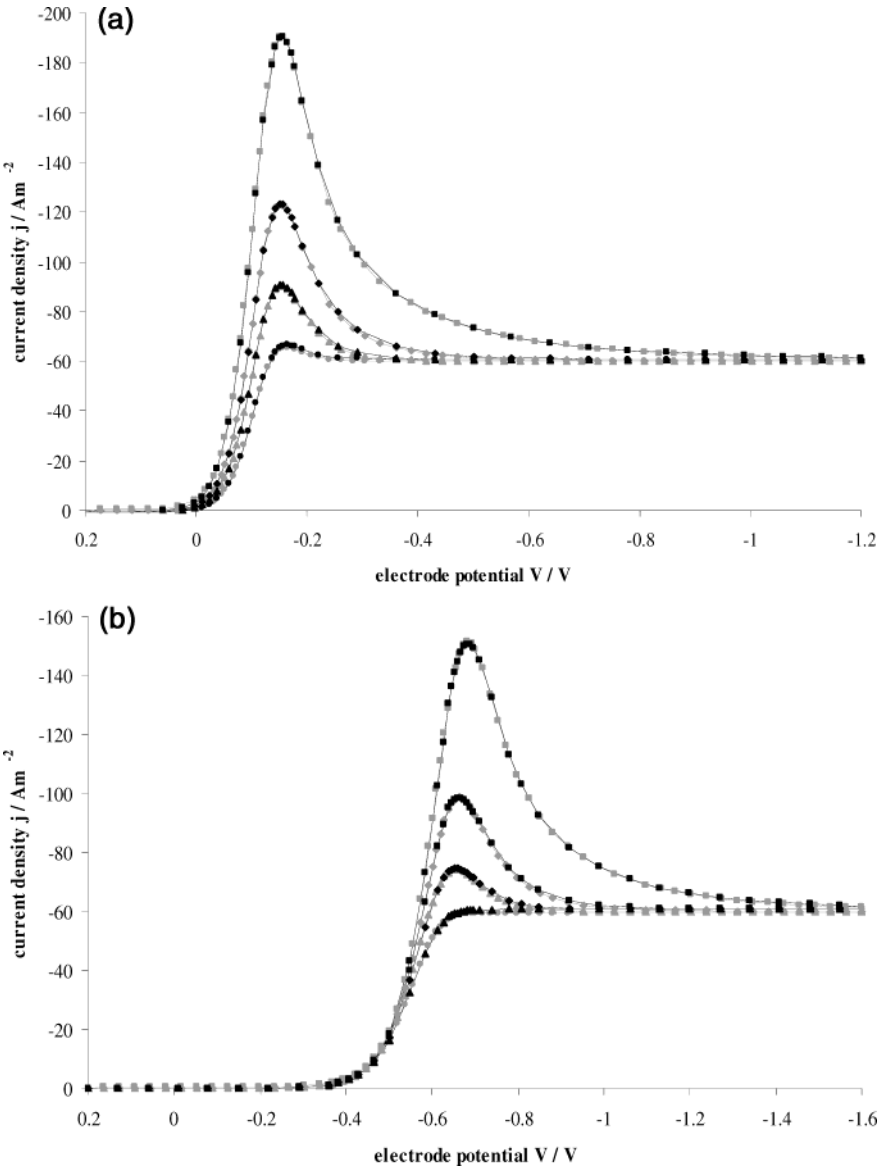

Figure 2. (a) Comparison of the current density response curves obtained with the 1D (gray lines) and AX approach (black lines) for system R, reversible electrode reaction. Scan rates: 0.4 (●), 1 (▲), 2 (◆), and 5 V s^{-1} (■). For visualization purposes, only ∼25% of the time points have been represented by a symbol. (b) Comparison of the current density response curves obtained with the 1D (gray lines) and AX approach (black lines) for system R, irreversible electrode reaction. Scan rates: 0.4 (●), 1 (▲), 2 (◆), and 5 V s^{-1} (■).

Table 6. Linear Regression Coefficient *a* for Electrolyte Systems A−F

	irreversible						reversible					
approach	A	B	C	D	E	F	A	B	C	D	E	F
AX	0.143	0.188	0.285	0.143	0.189	0.285	0.146	0.199	0.347	0.147	0.201	0.348
1D	0.164	0.204	0.294	0.165	0.206	0.294	0.180	0.230	0.361	0.180	0.230	0.361

Table 7. Linear Regression Coefficient *b* for Electrolyte Systems A−F

	irreversible						reversible					
approach	A	B	C	D	E	F	A	B	C	D	E	F
AX	0.660	0.547	0.303	0.656	0.538	0.298	0.719	0.630	0.339	0.715	0.621	0.330
1D	0.575	0.486	0.283	0.571	0.480	0.281	0.604	0.527	0.306	0.602	0.525	0.305

4, is based on finite volume techniques with upwind contributions for the convective ion transfer.[16] No preceding variable or coordinate transformations are performed. The Crank−Nicolson time integration scheme for MITRe simulations with transient

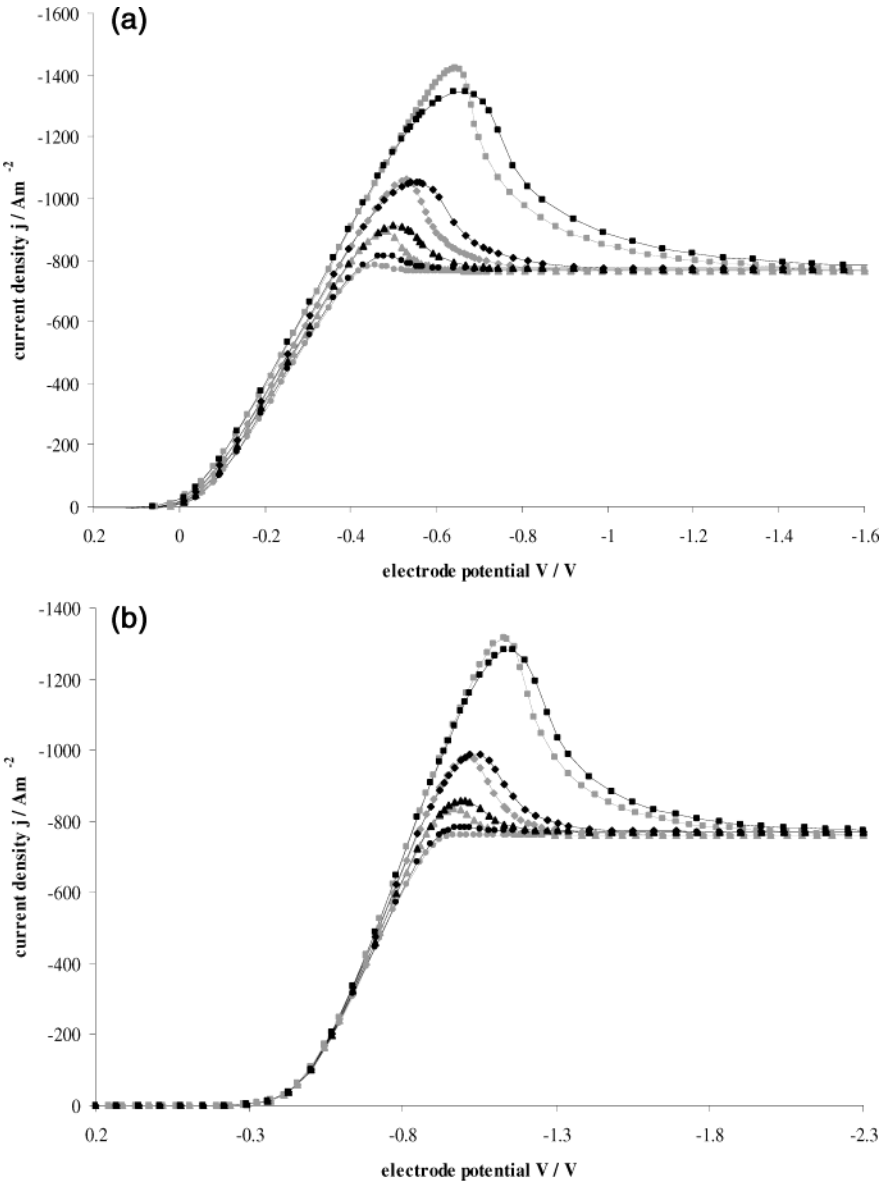

Figure 3. (a) Comparison of the current density response curves obtained with the 1D (gray lines) and AX approach (black lines) for system A, reversible electrode reaction. Scan rates: 0.4 (●), 1 (▲), 2 (◆), and 5 V s^{-1} (■). (b) Comparison of the current density response curves obtained with the 1D (gray lines) and AX approach (black lines) for system A, irreversible electrode reaction Scan rates: 0.4 (●), 1 (▲), 2 (◆), and 5 V s^{-1} (■).

excitation signals has been published more recently in ref 7. For each time step, a standard Newton−Raphson iteration method is used, and the resulting linear set of equations at each iteration is solved by a PGMRS algorithm.[22]

An axisymmetrical cross section of the electrolyte area adjacent to an RDE with radius $R_e = 1$ mm is considered. It is discretized with a hybrid triangular mesh,[23] featuring a fine structured layer adjacent to the electrode surface, and a coarse unstructured zone around this layer. The grid is plotted in Figure 1, with the symmetry axis to the left and the disk electrode surface at the bottom left. The axial element refinement of the structured layer is down to 4.0×10^{-9} m (with an element refinement factor of 1.1), enabling accurate modeling of the transient diffusion (−migration) layer phenomena. It was tested that further refinement does not bring enhanced accuracy. There is also a radial mesh refinement toward the electrode edge (also down to 4.0×10^{-9} m), to account for the small diffusion edge effect as described by Smyrl and Newman.[24] The outer regions of the structured layer and the unstructured zone adequately describe the electrolyte ohmic drop effects. Since the ohmic electrolyte drop is concentrated around the disk,[25] the mesh should (both radially and axially) expand to at least a few times the electrode radius. In this case, the axial and radial dimensions of the mesh were taken equal to 0.01 m. The total number of nodes is 9526 for 19 050 elements

The electrolyte fluid flow around the RDE, intervening in eq 1, is obtained from the analytical considerations of von Karman[26]

(22) Saad, Y.; Siam, J. *Sci. Comput.* **1993**, *14*, 461.
(23) Athanasiadis A. N.; Deconinck H. *Int. J. Numer. Methods Eng.* **2003**, *58*, 301.
(24) Smyrl, W. H.; Newman, J. J. *Electrochem. Soc.* **1971**, *118*, 1079.
(25) Newman, J. *Electrochemical Systems*, 2nd ed.; Prentice Hall: Englewood Cliffs, NJ, 1991; Chapter 18.

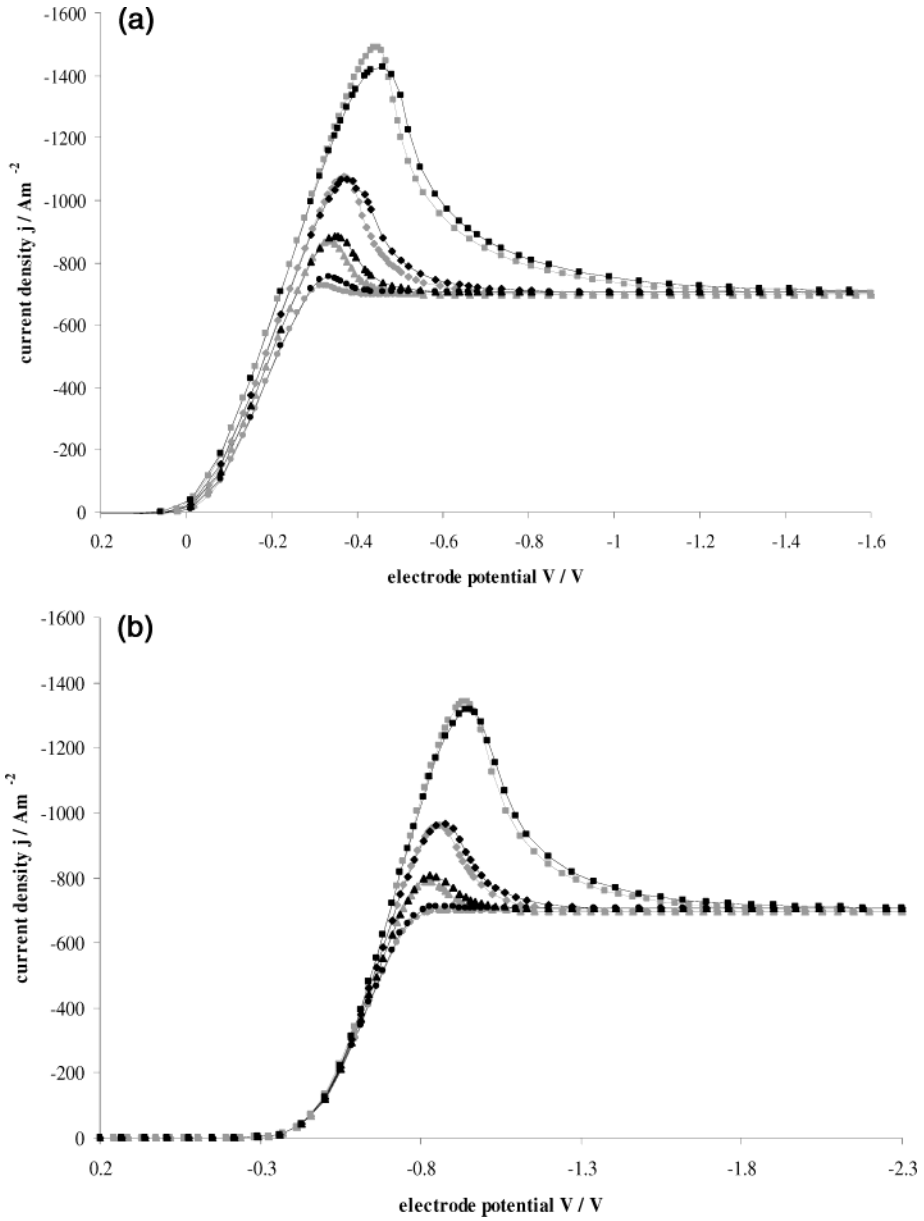

Figure 4. (a) Comparison of the current density response curves obtained with the 1D (gray lines) and AX approach (black lines) for system B, reversible electrode reaction. Scan rates: 0.4 (●), 1 (▲), 2 (◆), and 5 Vs^{-1} (■). (b) Comparison of the current density response curves obtained with the 1D (gray lines) and AX approach (black lines) for system B, irreversible electrode reaction. Scan rates: 0.4 (●), 1 (▲), 2 (◆), and 5 V s^{-1} (■).

and Cochran,[27] which yields for the first three terms in a series expansion:

$$v_z = (\Omega\nu)^{1/2}[-0.51023(\Omega/\nu)z^2 + 0.333(\Omega/\nu)^{1.5}z^3 - 0.103(\Omega/\nu)^2z^4] \quad (9)$$

$$v_r = r(\Omega\nu)^{1/2}[-0.51023(\Omega/\nu)2z + 0.333(\Omega/\nu)^{1.5}3z^2 - 0.103(\Omega/\nu)^2 4z^3] \quad (10)$$

where v_r and v_z are the radial and axial fluid flow velocity components (m s^{-1}), r and z represent the radial and axial coordinates (m), and ν holds for the kinematic viscosity (m^2 s^{-1}). The rotation speed Ω for simulations in this paper is kept fixed at 1000 rpm (= 104.71 rad s^{-1}). For all simulations, a time-dependent electrode potential V is imposed, while the electrolyte potential U at bulk phase side of the domain is kept constant at 0 V. The range of the imposed electrolyte potential V differs, depending on the electrolyte system and reaction kinetics, to ensure steady-state limiting current density conditions at the end of the process time: (a) 0.2 to −1.2 V for system R, reversible reaction type; (b) 0.2 to −1.6 V for systems A−F, reversible reaction type; (c) 0.2 to −1.6 V for system R, irreversible reaction type; (d) 0.2 to −2.3 V for systems A−F, irreversible reaction type.

The time step length Δt always corresponds to a voltage rise of 2 mV for all reaction types and each scan speed, which defines the values and number of the equidistant time steps in each case.

(26) von Karman, T.; Angew. Z. *Math. Mech.* **1921**, *1*, 233.
(27) Cochran, W. G. *Proc. Cambridge Philos. Soc. Math.* **1934**, *30*, 365.

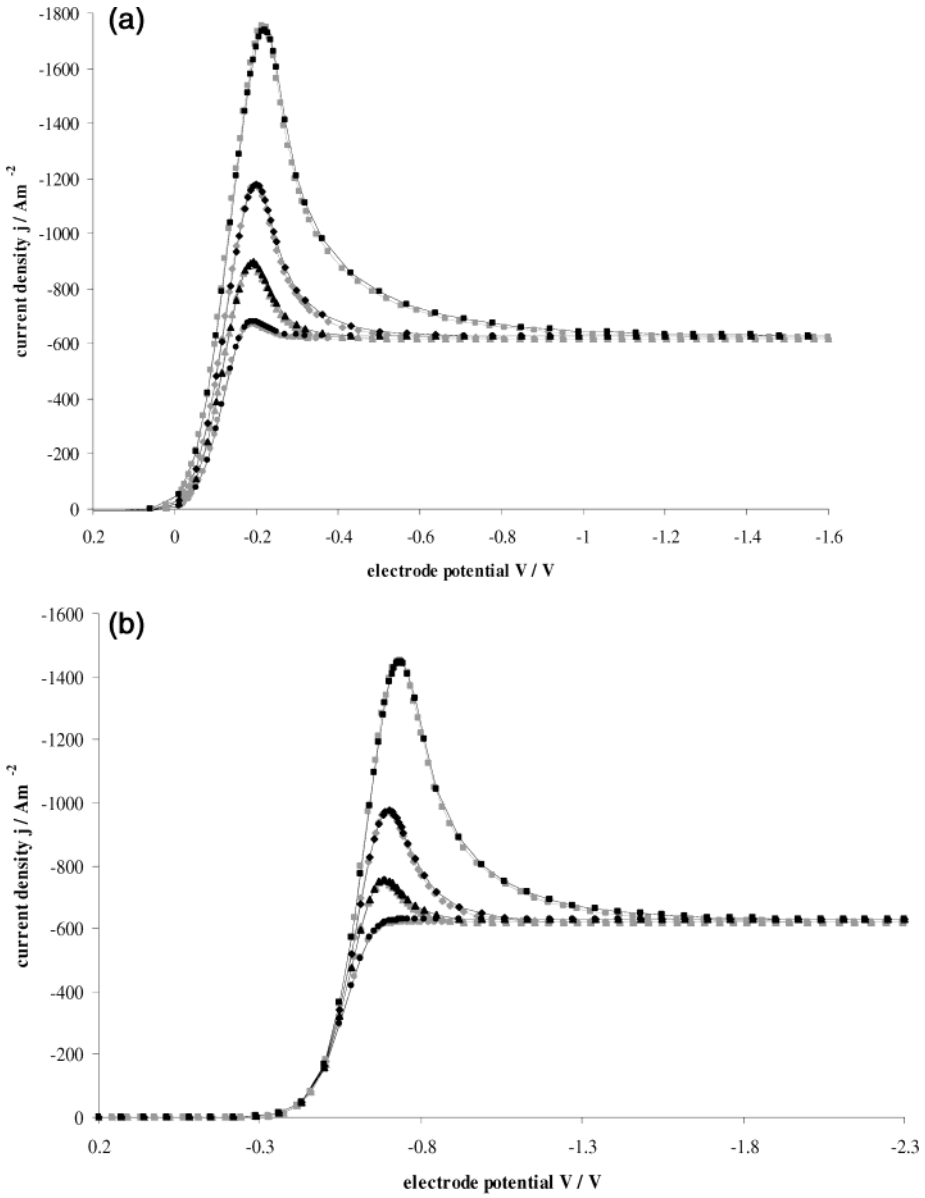

Figure 5. (a) Comparison of the current density response curves obtained with the 1D (gray lines) and AX approach (black lines) for system C, reversible electrode reaction. Scan rates: 0.4 (●), 1 (▲), 2 (◆), and 5 V s^{-1} (■). (b) Comparison of the current density response curves obtained with the 1D (gray lines) and AX approach (black lines) for system C, irreversible electrode reaction. Scan rates: 0.4 (●), 1 (▲), 2 (◆), and 5 V s^{-1} (■).

One-dimensional computations for the ion system of Table 1 have already been performed in ref 7, though only for the electrolyte composition of system R (Table 2). For comparison with the AX simulations, this type of computations will be repeated in this paper. To avoid systematic errors, the axial refinement should be the same as for the structured layer in the AX case (i.e., both refinement factor and element size adjacent to the electrode), and also the time steps are taken identical. The total length of the one-dimensional mesh is 1.0×10^{-4} m, sufficiently large to incorporate all diffusion and migration effects in the mass-transfer boundary layer. However, the ohmic drop outside this layer cannot be incorporated (due to the axisymmetrical nature of this phenomenon) and should be added analytically. The ohmic resistance R_{ohm} (Ω) of the electrolyte around an RDE is expressed by[25]

$$R_{ohm} = 1/4\sigma R_e \qquad (11)$$

and multiplication of this resistance by the numerically computed electrode current $I = j\pi R_e^2$ (A) yields the additional potential shift. The conductivity σ to be used in this equation is listed in Table 2 (for each ion system).

Peak Current Investigation. A very important characteristic to be obtained from linear voltammetry experiments and simulations is the peak current. Strutwolf and Schoeller demonstrated that, for sufficiently high scan speeds, the ratio of the peak current density j_P (A m^{-2}) and the limiting current density j_L is given by[28]

$$j_P/j_L = a\xi^{1/2} + b \qquad \xi = (nF\delta_N^2)/(RTD_1)\varpi \qquad (12)$$

with a, b linear regression coefficients. ω holds for the physical

(28) Strutwolf, J.; Schoeller, W. W. *J. Electroanal. Chem.* **1996**, *8*, 1034.

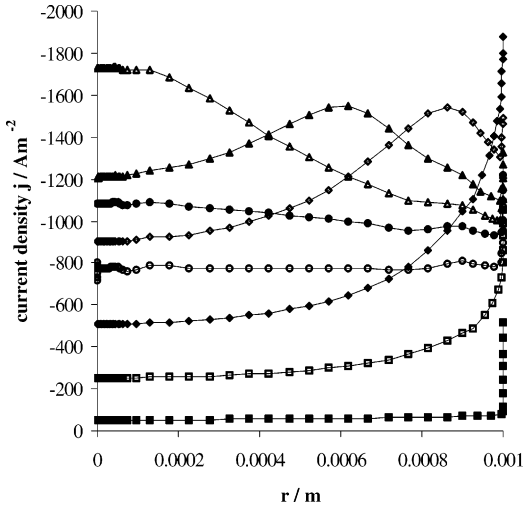

Figure 6. Current density distributions along the RDE for reversible system A at a scan rate of 5 V s^{-1}: $V = -0.038$ V, $t = 0.0476$ s (■); $V = -0.192$ V, $t = 0.0784$ s (□); $V = -0.36$ V, $t = 0.112$ s (◆); $V = -0.57$ V, $t = 0.154$ s (◇); $V = -0.668$ V, $t = 0.1736$ s (▲); $V = -0.745$ V, $t = 0.189$ s (△); $V = -0.85$ V, $t = 0.21$ s (●); $V = -1.606$ V, $t = 0.3612$ s (○).

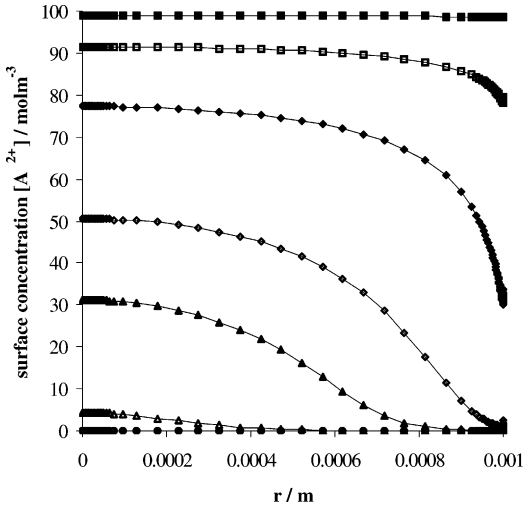

Figure 7. A^{2+} surface concentration distributions along the RDE for reversible system A at a scan rate of 5 V s^{-1}. Legend identical to Figure 6.

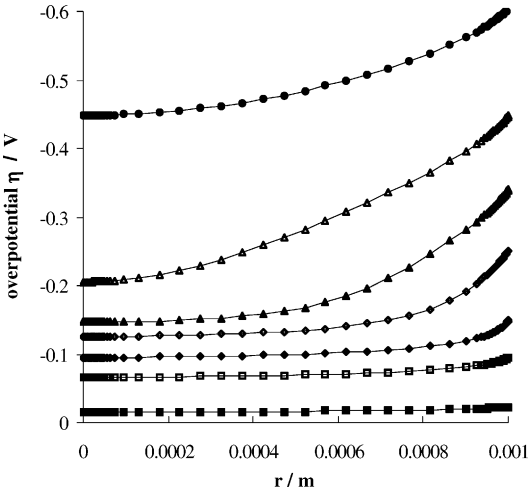

Figure 8. Overpotential distributions along the RDE for reversible system A at a scan rate of 5 V s^{-1}. Legend identical to Figure 6.

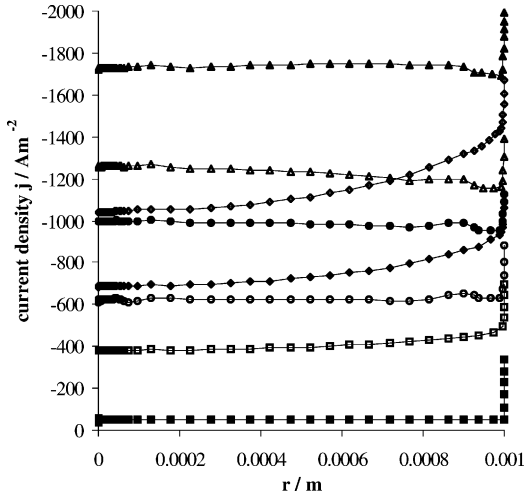

Figure 9. Current density distributions along the RDE for reversible system C at a scan rate of 5 V s^{-1}: $V = -0.01$ V, $t = 0.042$ s (■); $V = -0.08$ V, $t = 0.056$ s (□); $V = -0.115$ V, $t = 0.063$ s (◆); $V = -0.15$ V, $t = 0.07$ s (◇); $V = -0.22$ V, $t = 0.084$ s (▲); $V = -0.297$ V, $t = 0.0994$ s (△); $V = -0.36$ V, $t = 0.112$ s (●); $V = -1.606$ V, $t = 0.3612$ s (○).

scan speed (V/s) and ξ for the dimensionless one. D_1 is the diffusion coefficient of the A^{2+} ion, and n *is* the number of electrons exchanged in the electrode reaction. In eq 12, the Nernst diffusion layer thickness δ_N is computed from

$$\delta_N = 1.6118 D_1^{1/3} \nu^{1/6} \Omega^{-1/2} \qquad (13)$$

Based on simulations for several scan speeds, the ratio j_P/j_L can be calculated as a function of $\xi^{1/2}$, enabling one to obtain the linear regression coefficient *a*. In this paper, simulations are always performed for four different scan rates ω, i.e., 0.4, 1, 2, and 5 V/s. Since eq 12 only holds for sufficiently high scan rates (see Table 5), the lowest scan rate is not retained for fitting the linear regression coefficients *a* and *b*.

RESULTS AND DISCUSSION

Validation of the Axisymmetrical Linear Voltammetry Simulations. The accuracy of steady-state AX simulations for MITRe models was investigated extensively in ref 16, for two systems with a distinct amount of supporting electrolyte. A Cranck−Nicolson time integration scheme was proven to yield accurate 1D MITRe simulation results in ref 7. It remains to be tested whether this time integration scheme can also provide accurate results for AX simulations. To this purpose, ion system R (Table 2) is selected, and simulations are performed for different scan rates ω, assuming both the reversible and irreversible reaction types from Table 3. The advantage of using ion system R lies in the very uniform current density distribution, due to the very low reaction ion bulk concentration, which severely restricts the current densities that can be attained. Hence, from a theoretical point of view, the AX and 1D simulations should give nearly identical results. The current response for this system is plotted in Figure 2a and b, and there is indeed excellent agreement between results of the AX and the 1D approach. Both peak currents and the currents at the end of the process time (approaching very closely the steady-state limiting current) match below 1.2% of difference. The linear regression coefficient *a* shows

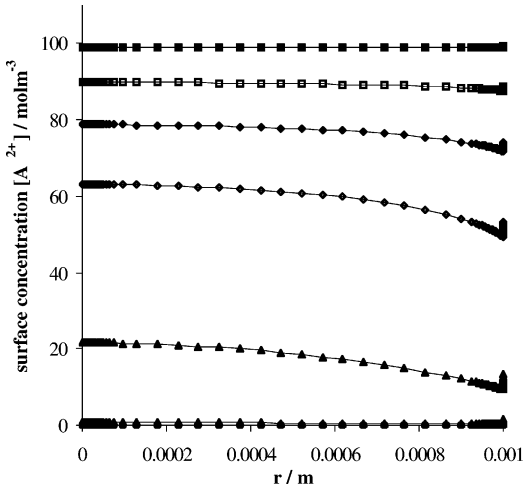

Figure 10. A^{2+} surface concentration distributions along the RDE for reversible system C at a scan rate of 5 V s^{-1}. Legend identical to Figure 12.

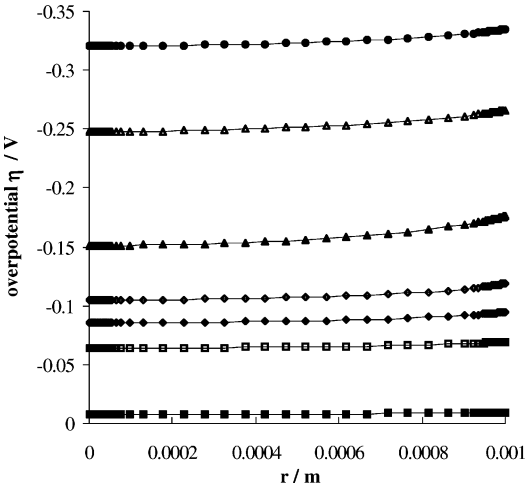

Figure 11. Overpotential distributions along the RDE for reversible system C at a scan rate of 5 V s^{-1}. Legend identical to Figure 12.

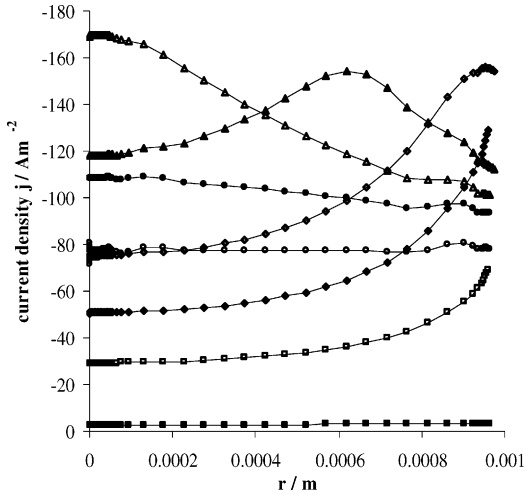

Figure 12. Current density distributions along the RDE for reversible system D at a scan rate of 5 V s^{-1}: $V = -0.01$ V, $t = 0.042$ s (■); $V = -0.22$ V, $t = 0.084$ s (□); $V = -0.36$ V, $t = 0.112$ s (◆); $V = -0.5$ V, $t = 0.14$ s (◇); $V = -0.661$ V, $t = 0.1722$ s (▲); $V = -0.752$ V, $t = 0.1904$ s (△); $V = -0.85$ V, $t = 0.21$ s (●); $V = -1.606$ V, $t = 0.3612$ s (○).

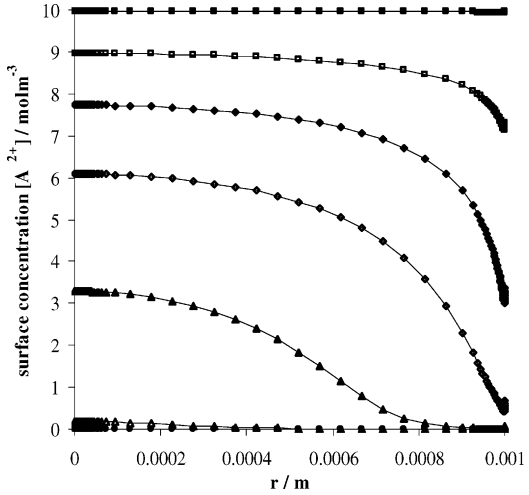

Figure 13. A^{2+} surface concentration distributions along the RDE for reversible system D at a scan rate of 5 V s^{-1}. Legend identical to Figure 12.

agreement below a relative error of 2.5% (Table 5). The small differences are partly due to the numerical method (and triangular mesh) that is being used, but also due to the radial edge diffusion effect, as described by Smyrl and Newman.[24]

Comparison between One-Dimensional and Axisymmetrical Simulations. AX as well as 1D simulations are performed for all process conditions as listed in Tables 2 (electrolyte composition) and 3 (electrode kinetics). For each case, the linear regression coefficient *a* from eq 10 is determined, based on the simulated results for three different scan rates. An overview is given in Table 6.

Only in case an excess of supporting electrolyte is present (system C), the 1D result matches very closely the AX result (see Figure 5), the *a* coefficient differing by ∼3% (Tables 6 and 7). For system B, containing only a limited amount of supporting electrolyte, the discrepancy becomes significant (see Figure 4), and the *a* coefficient differs between 8 (irreversible) and 13% (reversible reaction type). When supporting electrolyte is nearly entirely absent (system A, Figure 3), important systematic errors are generated when using the 1D approach instead of the AX one. The difference in *a* coefficient amounts to 18% for the reversible reaction type. Table 6 also reveals that the discrepancy between 1D and AX results is more pronounced for systems with reversible reaction kinetics. A direct comparison between the current response for the 1D and AX approaches reveals important current response differences for electrolyte systems A and B (Figures 3 and 4), which are entirely due to the highly nonuniform local process conditions over the electrode surface. For system C, the current response from the 1D and AX approaches nearly collapse. For system A, the peak current is over 5% lower in the AX case compared to the 1D case (highest scan rate, reversible reaction kinetics). The peak broadening is above 20% (for each scan rate, reversible reaction kinetics), and the current peak is shifted toward more negative electrode potentials by ∼50 mV (for each scan rate, both reaction types). The results for systems D−F, including the observed discrepancies between between 1D and AX results, are nearly identical to those for systems A−C (apart for the limiting current densities being 1 order of magnitude lower). This is reflected in the *a* and *b* coefficients for systems D−F, being nearly identical to those for systems A−C, respectively (Tables 6 and

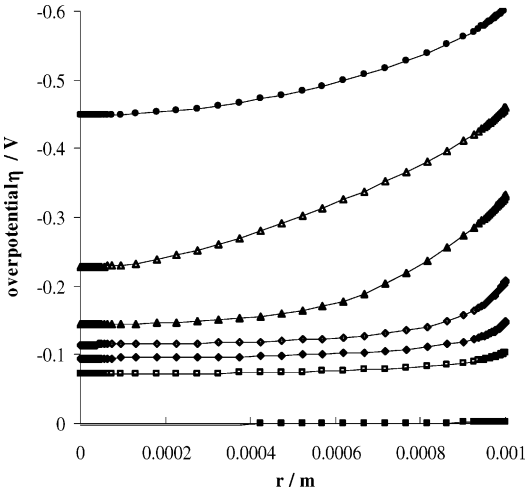

Figure 14. Overpotential distributions along the RDE for reversible system D at a scan rate of 5 V s^{-1}. Legend identical to Figure 12.

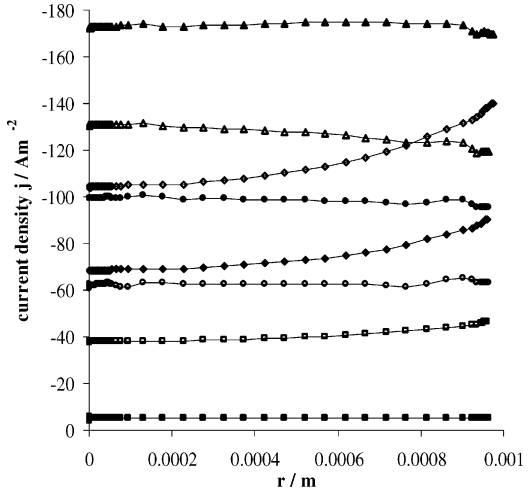

Figure 15. Current density distributions along the RDE for reversible system F at a scan rate of 5 V s^{-1}: $V = -0.01$ V, $t = 0.042$ s (■); $V = -0.08$ V, $t = 0.056$ s (□); $V = -0.115$ V, $t = 0.063$ s (◆); $V = -0.15$ V, $t = 0.07$ s (◇); $V = -0.22$ V, $t = 0.084$ s (▲); $V = -0.29$ V, $t = 0.098$ s (△); $V = -0.36$ V, $t = 0.112$ s (●); $V = -1.508$ V, $t = 0.3416$ s (○).

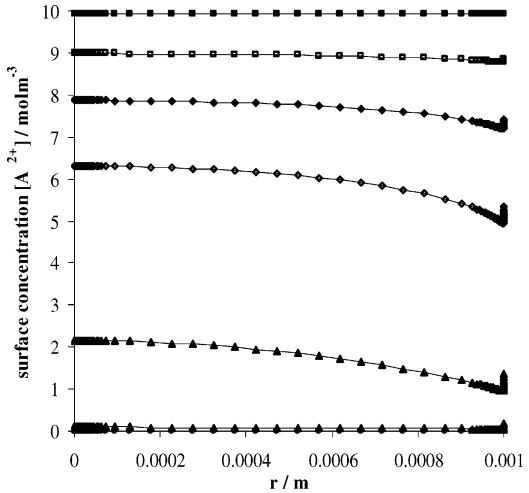

Figure 16. A^{2+} surface concentration distributions along the RDE for reversible system F at a scan rate of 5 V s^{-1}. Legend identical to Figure 12.

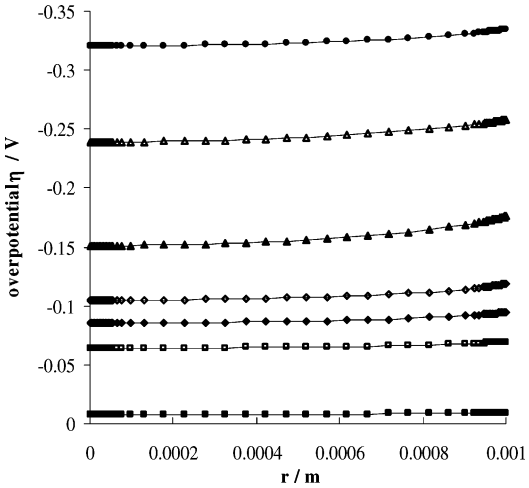

Figure 17. Overpotential distributions along the RDE for reversible system F at a scan rate of 5 V s^{-1}. Legend identical to Figure 12.

Table 8. Limiting Current Density j_L (A m^{-2}) for Electrolyte Systems R and A−F

approach	A	B	C	D	E	F	R
AX	−771	−705	−627	−77.1	−70.5	−62.7	−60.8
1D	−762	−697	−619	−76.3	−69.8	−62.0	−60.1

7). Hence, the discrepancy between the AX and 1D results is mainly dependent on the transference number, while the ionic strength influence is very restricted. Due to the similarity with systems A−C, the current response for systems D−F has not been plotted.

The most relevant local process conditions (current density j, A^{2+} concentration, overpotenial η) are plotted in Figures 6−8 (system A) and 9−11 (system C), for the highest scan speed (5 V/s) and reversible reaction kinetics. In Figure 6, the nonuniformity of the current density distribution is gradually increasing from $t = 0.0476$ s to $t = 0.112$ s. This is due to a higher driving force (overpotential η) near the boundary of the RDE (Figure 8), invoking lower A^{2+} surface concentrations in this region (Figure 7). Later in time the uniformity of the current density distribution is increasing again and the maximum value of the current density gradually moves toward the center of the RDE (Figure 6). This is due to the mass-transfer limiting conditions that have been attained near the RDE edge (Figure 7). For system C (Figures 9−11), the migrational edge effect influence is no longer important and an almost uniform current density distribution is obtained at each time step (Figure 9). The current density distributions in Figures 6, 9, and 12 show some numerical noice near the symmetry axis, which is not uncommon when using FVM or FEM for convection diffusion problems in AX configurations.

For each system, the radial diffusion edge effect is clearly visible (Figures 6−17), reflected by the sharp variation of local process conditions very close to the electrode edge. The impact of this effect on the total current remains, however, very restricted[16,24] (<1%).

The steady-state limiting currents obtained from the AX en 1D approach match very well (below 1.2%) for each system. This is illustrated in Table 8, where the simulated steady-state limiting currents are approximated by the response current at the end of the simulated process time). It is noted that the limiting currents

Table 9. Values for Logarithmic Regression Coefficients *r*, *s*, *t*, and *u*

	irreversible				reversible			
approach	*r*	*s*	*t*	*u*	*r*	*s*	*t*	*u*
AX	−0.061	0.116	0.153	0.724	−0.087	0.103	0.168	0.805
1D	−0.056	0.139	0.125	0.629	−0.078	0.142	0.129	0.668

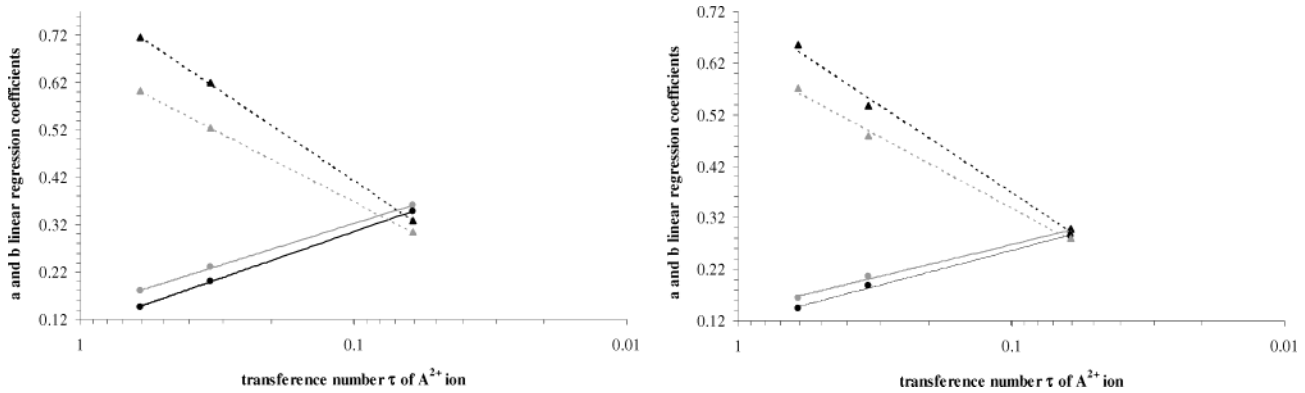

Figure 18. Linear regression coefficients*a* (full line, ●) and *b* (dashed line, ▲) as a function of the A^{2+} transference number. 1D results in gray, AX results in black. Results for reversible reaction kinetics to the left; irreversible reaction kinetics to the right.

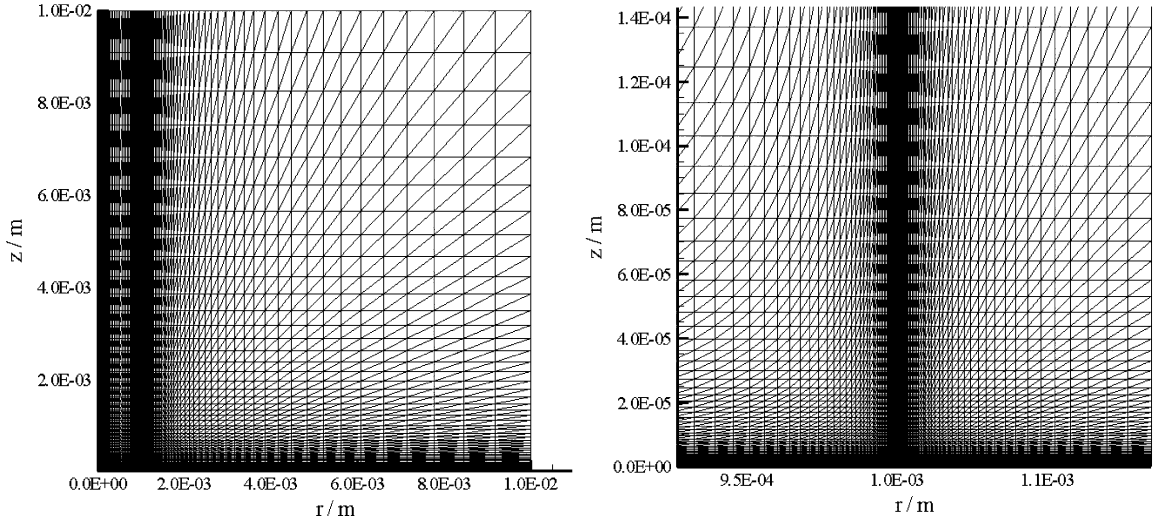

Figure 19. Structured triangular mesh around the RDE (axis of symmetry at $r = 0$ m, disk extending to $r = 0.01$ m). Zoom around the disk edge is plotted at the right.

for system A−C (or D−F) differ significantly. This is explained by the migrational effect on the A^{2+} ion transport in the diffusion boundary layer.

The migrational influence upon the peak current density can be encaptured in an empirical correlation. Since the results from Tables 6 and 7 indicate that the ionic strength has very little influence, a simple logarithmic depence of the *a* and *b* regressions coefficients on the transference number τ is suggested:

$$a = r \log \tau + s \qquad b = t \log \tau + u \tag{14}$$

Equation 14 (combined with eqs 12 and 13) allows one to predict in a fast manner the peak current for arbitrary electrolyte systems without an excess of supporting electrolyte, provided that mass transfer is dominated by one single reacting species as in eq 5 (and that this species has a charge that is of opposite sign compared to the reaction current density). As a consequence, this equation can also be used to estimate the systematical error that is made when performing 1D simulations for a linear voltammetry experiment. The logarithmic regression coeffcients are obtained from fitting peak current results for the entire set of electrolyte systems A−F (Table 9). It is illustrated in Figure 18 that the logarithmic correlation from eq 14 allows a very accurate fitting of the sample data.

Computational Efforts. A complete AX linear voltammetry simulation using the hybrid mesh from Figure 2 requires a CPU time ranging from 190 (system C, reversible, scan rate 1 V/s) to 410 min (system A, irreversible, scan rate 5 V/s) for, respectively, 259 and 358 time/potential steps (on a 2.4-GHz, *2* GB RAM PC). Between 4 and 20 Newton iterations are required for each time step to reach a sufficient convergence level. These values are to be compared to the computational efforts for the 1D approach, where CPU times for an entire linear voltammetry simulation require only ∼30 s.

The advantage of using a hybrid mesh can be easily illustrated by comparing the CPU times with those for a simulation that is based on a structured mesh. Figure 19 shows a structured triangular mesh with the same specifications (i.e., axial and radial refinement factor and element size adjacent to the electrode) as the structured layer of the hybrid triangular mesh adjacent to the RDE. For this mesh, the total number of nodes is 44 880 for 89 758 elements. The structured mesh has ∼5 times more elements and nodes than the unstructured one, resulting in a CPU time of 1020 min (system C, reversible, scan rate 1 V/s). This implies that the use of a hybrid mesh can reduce CPU times by a factor of 5 or higher.

CONCLUSION

The simulation results as presented in this paper illustrate that a 1D approach for computing transient behavior of electrochemical systems at an RDE produces non-negligible systematic errors. Only for electrochemical systems with an excess of supporting electrolyte (systems R, C, and F) are the transient current response obtained from the 1D and AX approaches nearly identical. For systems with lack of supporting electrolyte (system A and D), the errors on simulated peak current densities easily amount to 5% and more, with important peak broadening (>20%) and a peak shift toward more negative electrode potentials of ∼50 mV. This puts a severe restriction on the validity of electrochemical kinetic data that are extracted from comparing transient 1D simulations to RDE experiments (cyclic voltammetry, potential, current steps, etc.). It is also demonstrated that the peak current for arbitrary electrolyte systems without an excess of supporting electrolyte, involving one single reacting species, can be obtained from an empirical correlation. This allows one to estimate the systematical error that is made when performing 1D simulations for a linear voltammetry experiment at an RDE.

An unsimplified AX numerical approach can provide an accurate solution for any MITRe model, and any type of transient experiment, but at the cost of considerable CPU time. Increasing PC computing performances and more advanced numerical schemes (e.g., higher order time integration) can significantly reduce the CPU time, but in the short term they are unlikely to provide the required tools to gain, for example, 2 orders of magnitude (i.e., from hours to minutes) in CPU time, which would be required for a fast AX investigation or parameter fitting of MITRe models. Nevertheless, this paper illustrates that the use of hybrid meshes is a valid strategy to reduce CPU times by at least a factor of 5. As an implication, FVM or FEM approaches are to be favored over the FDM for solving MITRe models in 2D or AX configurations, since the FDM is by definition based on a structured mesh.

ACKNOWLEDGMENT

The Vrije Universiteit Brussel sponsored this research project under project G.O.A. No. 11.

Received for review February 4, 2004. Accepted July 8, 2004.

AC049804D